Soft fragmentation of carbon monoxide by slow highly charged ions

E. Wells,[1,2,*] T. Nishide,[3] H. Tawara,[2,4,†] R. L. Watson,[5] K. D. Carnes,[2] and I. Ben-Itzhak[2]
[1]*Department of Physics, Augustana College, Sioux Falls, South Dakota 57197, USA*
[2]*J.R. Macdonald Laboratory, Department of Physics, Kansas State University, Manhattan, Kansas 66506, USA*
[3]*Graduate School of Science, Tokyo Metropolitan University, Tokyo 192-0397, Japan*
[4]*National Institute for Fusion Sciences, Nagoya 464-01, Japan*
[5]*Department of Chemistry, Texas A&M University, College Station, Texas 77843, USA*
(Received 17 August 2007; revised manuscript received 30 April 2008; published 12 June 2008)

The fragmentation pattern and corresponding kinetic energy release distributions from carbon monoxide after collisions with slow, highly charged ions (C^{6+} at $v=0.8$ a.u. and Ar^{11+} at $v=0.39$ a.u.) are reported. Correlated measurements of the projectile final charge state and all charged molecular fragments were obtained using a coincidence time-of-flight technique coupled to projectile charge state separation. Fragmentation branching ratios for the dominant electron capture processes in these collisions are similar to those resulting from ionization by fast highly charged projectiles. This result can help simplify simulations of astrophysical or artificial plasma environments, as the branching ratio may be considered essentially constant for both electron capture and ionization as long as the relevant impact parameter is large.

DOI: 10.1103/PhysRevA.77.064701 PACS number(s): 34.50.Gb

Charge exchanging collisions between highly charged ions (HCIs) and neutral molecular targets are a significant process in astrophysical settings [1], such as planetary atmospheres [2,3], comets [4–7], and interstellar clouds [8]. Carbon monoxide, in turn, is an important part of the molecular clouds surrounding galaxies [9], comet tails [10,11], and the atmospheres of Titan [12] and Triton [13]. As a result, it is desirable to know accurate electron capture cross sections and fragmentation branching ratios of HCI-CO collisions for modeling purposes [14]. The same information is also necessary to understand HCI-molecule collisions in various artificial plasma environments [15], including fusion devices [16].

We have previously reported cross sections, fragmentation branching ratios, and the kinetic energy release (KER) upon dissociation of CO colliding with fast highly charged ions [17–19] and protons over a wide range of velocities [20]. These collision studies, and others like them [21–28], are interesting because the KER and the branching ratios give insight into the dynamics associated with the transient excited states of the molecular ion. With the exception of the low-velocity proton impact data reported in Ref. [20], these projectiles do not model very well the solar wind or magnetospherically confined ions that are often of interest in astrophysical settings. Highly charged ions with energies in the few keV per charge state (q) regime, however, are an important part of the fast solar wind [29]. In fact, highly charged carbon ions are the most abundant species in the solar wind save for protons and alpha particles [29].

In this Brief Report, we present measurements of the fragmentation branching ratio and KER as a result of slow ($v=0.8$ a.u.) C^{6+} and ($v=0.39$ a.u.) Ar^{11+} ions colliding with CO. When these results are compared to each other and to previous data, it is apparent that the CO fragmentation pattern remains approximately constant over a wide range of projectile charges and velocities, regardless of the specific electron removal mechanism. The qualitative explanation for this is that due to the many-electron nature of the target, the interaction strength, $\frac{q}{vb}$ (q is the projectile charge and b is the impact parameter) [30] is roughly the same for any process removing a specific number of electrons, and thus similar excited states of the molecular ion are populated yielding similar branching ratios. Stated another way, as $\frac{q}{v}$ increases, the value of the impact parameter increases correspondingly and the collision remains "soft." This result is contrary to earlier results obtained from collisions between highly charged ions and H_2 targets, which display a more complicated relationship between impact parameter and collision velocity [31–33]. Even in the 14-electron CO target, if you select a process that has a small impact parameter, such as capture at high velocity or ionization at low velocity, variation in the branching ratio is observed [20,24]. For the one- or two-electron processes that dominate the cross section, and are therefore of most interest for astrophysical modeling, the CO fragmentation branching ratios appear to remain quite constant as $\frac{q}{v}$ changes. In contrast, the KER distributions show more variation as the interaction strength is varied. Finally, we report the distribution of projectile charge states resulting from these collisions and compare the results to a model calculation.

The apparatus, experimental technique, and data analysis methods are described elsewhere [20,34,35] and are only summarized here. A beam of HCI produced by the KSU-CRYEBIS [36] was accelerated using the source platform voltage, charge separated by an analyzing magnet, and directed toward the target region where it intersected a jet of carbon monoxide. The effusive molecular jet localized the target in the strong uniform extraction field of a two-stage Wiley-McLaren [34,37] spectrometer which accelerated all recoil ions toward a microchannel plate (MCP) detector. The projectiles were charge analyzed after the collision by an

*eric.wells@augie.edu
†Present address: Max-Planck-Institut für Kernphysik, D-69029 Heidelberg, Germany.

TABLE I. Relative cross sections of all measured final states of the molecular ion in coincidence with the final projectile charge state for C^{6+}+CO collisions at $v=0.8$ a.u. All results are normalized to the dominant $C^{5+}+CO^{+}$ final state.

Channel	C^{5+}	C^{4+}	C^{3+}
CO^{+}	100		
$C^{+}+O$	9.9 ± 4.6		
$C+O^{+}$	9.4 ± 3.2		
CO^{2+}	2.7 ± 0.4	0.3 ± 0.06	
$C^{2+}+O$	4.2 ± 1.0	2.5 ± 0.6	
$C^{+}+O^{+}$	26.1 ± 3.5	0.93 ± 0.35	
$C+O^{2+}$	2.1 ± 0.5	1.67 ± 0.4	
$C^{3+}+O$	3.1 ± 0.30	1.2 ± 0.20	
$C^{2+}+O^{+}$	6.4 ± 0.85	4.4 ± 0.6	
$C^{+}+O^{2+}$	1.9 ± 0.37	1.2 ± 0.23	
$C+O^{3+}$	1.4 ± 0.24	0.53 ± 0.14	
$C^{3+}+O^{+}$	0.26 ± 0.066	0.34 ± 0.09	
$C^{2+}+O^{2+}$	2.2 ± 0.32	2.3 ± 0.35	
$C^{+}+O^{3+}$	0.18 ± 0.05	0.16 ± 0.05	
$C+O^{4+}$	0.31 ± 0.013	0.14 ± 0.03	
$C^{4+}+O^{+}$	0.0006 ± 0.0004	0.016 ± 0.008	0.017 ± 0.008
$C^{3+}+O^{2+}$	0.51 ± 0.09	1.0 ± 0.17	0.03 ± 0.01
$C^{2+}+O^{3+}$	0.53 ± 0.09	1.1 ± 0.18	0.04 ± 0.02
$C^{+}+O^{4+}$	0.0036 ± 0.002	0.012 ± 0.005	0.026 ± 0.012
$C^{4+}+O^{2+}$	0.0027 ± 0.0012	0.010 ± 0.006	0.008 ± 0.005
$C^{3+}+O^{3+}$	0.25 ± 0.08	0.74 ± 0.22	0.10 ± 0.04
$C^{2+}+O^{4+}$	0.035 ± 0.019	0.11 ± 0.059	0.092 ± 0.050

electrostatic deflector as well as by the extraction fields in the spectrometer itself. The recoil ions produced in a single collision were identified using a coincidence-time-of-flight technique [34] using a common stop from the projectile detector.

The final charge state of the projectile was determined using a two-dimensional position sensitive MCP detector located 1.3 m downstream from the target. The 1.3 m flight length for the projectiles after leaving the target region made for good separation of charge states on the projectile detector ($\sim$1 cm), which has a resolution of 0.2 mm. The determination of the projectile charge state was made in off-line analysis of the event-by-event data by first requiring a coincidence with a particular recoil ion to reduce the random projectile yield. The two-dimensional projectile position was then projected onto the axis parallel to the deflector field and fit with multiple Gaussians to determine the projectile charge state yield in association with that recoil ion (ions) channel. As described in Refs. [17,18,20,34,35], the data were corrected for double collisions, detection efficiency less than 1.0, and contaminant beam charge states.

The main results of the measurement with C^{6+} projectiles are given in Table I. (Similar results for $v=0.39$ Ar^{11+} and $v=9.85$ Ar^{14+} collisions with CO may be found in Ref. [39].) At the collision velocities under study, electron capture to the highly charged projectile is dominant and direct target ionization is negligible [20,25]. Single electron capture is the largest channel, followed by the $C^{+}+O^{+}$ channel (about four times less likely) and the order-of-magnitude smaller $C^{+}+O$ and $C+O^{+}$ channels. Two other main features of the data are apparent. First, when multiple electrons are removed from the target, charge-symmetric dissociation is the favored dissociation pathway. This phenomenon has been observed in other collision systems [17,22,38] and is understood to be a consequence of the ability of the electron cloud to rearrange quickly compared to the much slower nuclear motion in the dissociation process. For charge asymmetric channels, the production of (multiply ionized) carbon ions is generally favored over production of the corresponding oxygen ions, most likely because oxygen has a larger binding energy.

The branching ratios shown in Table I are similar to the branching ratios measured in other experiments over a range of projectile q and v [17,19,20] in which direct target ionization is usually dominant and always non-negligible. To examine if the trend, shown in Fig. 1, remained consistent as the value of $\frac{q}{v}$ increased, we also measured Ar^{11+}+CO collisions at $v=0.39$ a.u., for which the projectile $\frac{q}{v}$ reaches 28 [39]. Some change in the branching ratio was observed, but the changes were generally less than about 10% of the total while $\frac{q}{v}$ changes by nearly two orders of magnitude in the range of experiments shown. The relative change in the main channels, though larger ($\lesssim$50%), is still slow for the wide range of q/v. One might expect that as the ratio of projectile $\frac{q}{v}$ increases, the branching ratios would shift toward multiply charged fragments. Somewhat counterintuitively, the amount of "soft" capture (i.e., CO^{+}) increases as $\frac{q}{v}$ increases from 7.5 to 28. The qualitative explanation for this is that the increase in q is accompanied by an impact parameter increase such that the interaction strength needed to remove the electrons is preserved. Therefore, the branching ratios remain fairly constant over the range of collisions studied. If, however, one experimentally isolates a small impact parameter process, a "hard" collision is observed. These collisions may well involve inner-shell electrons, leading to autoionization of the target and increased fragmentation. This is dramatically illustrated by a reanalysis of data [39] first reported in Ref. [24] to obtain the branching ratios from electron capture induced by 97 MeV Ar^{14+} ions. For example, in that experiment [24], the $C^{+}+O^{2+}$ was favored over the $C^{2+}+O^{+}$ dissociation by about 36%. Our results (see Table I) favor the $C^{2+}+O^{+}$ channel by a factor of 3.4.

The second main point that is apparent from Table I involves the final charge state of the projectile. The presence of highly charged recoil ions (up to six electrons removed even though we only measure projectiles up to $q=3$) indicate that multiple electron capture is likely to be followed by a fast autoionization of the projectile, specifically faster than the transit time of the projectile through the analyzer, i.e., less than about 50 ns. Radiative stabilization of the projectile, in contrast, is a relatively rare outcome. For example, radiative stabilization only occurs 3.3% of the time for the main double capture channel yielding $C^{+}+O^{+}$ dissociation in these collisions. The propensity of the projectile to autoionize following multiple electron capture would seem to indicate that the electrons are predominately captured into a doubly excited state of the projectile. To verify this assumption, we have used the extended over-barrier model (EOBM) [40] to

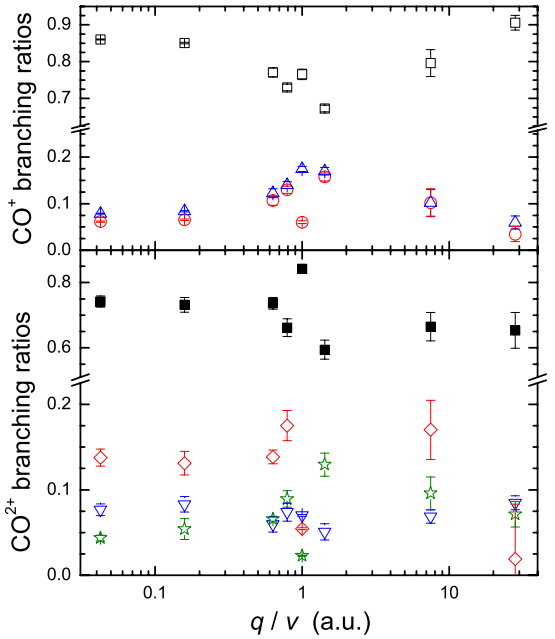

FIG. 1. (Color online) Fragmentation branching ratios from the transient excited states of CO^+ (top) and CO^{2+} (bottom) as a function of $\frac{q}{v}$. Fragmentation channels are denoted by CO^+ (□), $C^+ + O$ (△), $C + O^+$ (○), $C^+ + O^+$ (■), CO^{2+} (▽), $C^{2+} + O$ (◇), and $C + O^{2+}$ (★). Besides the present results at $q/v = 7.5$ (C^{6+}) and 28 (Ar^{11+}), the other projectiles include 1 MeV/u F^{4+}, F^{9+}, B^{5+}, and H^+, and 25 keV H^+. Except for the 25 keV H^+ impact, in which the fragmentation branching ratio shown here includes both capture and ionization, the results from the previously reported measurements [17,19,20] represent direct ionization of the CO target.

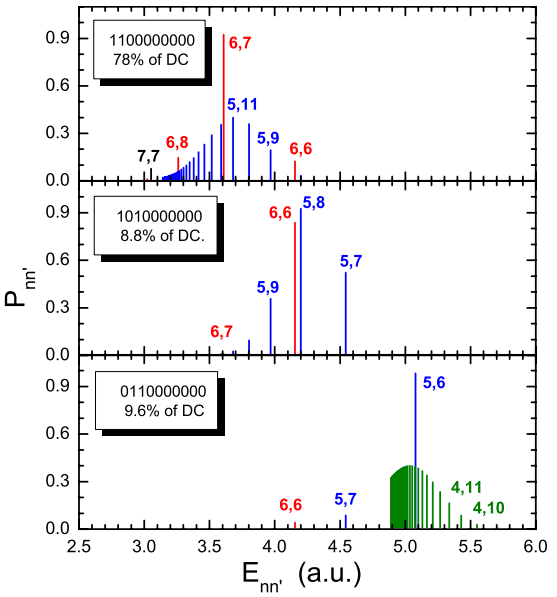

FIG. 2. (Color online) The probability for double electron capture (DC) to populate the projectile principle quantum states n and n' according to EOBM calculations of $Ar^{11+} + CO$ collisions at $v = 0.39$. The probabilities are plotted versus the energy of the (n,n') state. The string of numbers in the legend indicates which of the 10 non-K-shell electrons are captured. For example, in the top panel, the two least tightly bound electrons are captured from CO. The EOBM estimates that this occurs 78% of the time. Colors are associated with a given n: $n=4$ (green), 5 (blue), 6 (red), 7 (black).

calculate the probability of capture into a particular set of projectile states for the $Ar^{11+} + CO$ collisions discussed earlier. The results of these calculations, shown in Fig. 2, indicate that the first electron will usually be captured into $n = 6 \pm 1$, with the second electron captured in a state n' ranging from 4 to 11. Many of these states autoionize rapidly, accounting for the measured projectile charge distribution. Results for carbon projectiles showed similar trends.

While the branching ratios are fairly insensitive to changes in the projectile $\frac{q}{v}$, the KER distributions are more sensitive probes of the excited electronic states of the parent molecular ion. Figure 3 illustrates how the KER distributions change with either projectile velocity or the presence of projectile electrons. The recent paper by Rajput and Safvan [28] has examined the KER distributions from $Ar^{8+} + CO$ collisions at $v = 1.1$ a.u., with particular attention to the $CO^{(4-6)+}$ dissociation channels. Our experiment obtained similar data, although we note in passing that unlike the previous result [28], we observe the $C^{4+} + O^{2+}$ channel in both the carbon and argon collision systems. The KER distributions of the various fragmentation channels are relegated to the EPAPS material associated with this Brief Report [39]. Nearly all of the KER distributions have components that differ significantly from a simple Coulomb explosion picture in agreement with previous observations with higher energy resolution that allowed identification of some of these states (see Ref. [27], and references therein). Further evidence that many excited electronic states of the transient molecular ion are populated is given by the EOBM results, which indicate that about 20% of the double capture process involves inner-shell electrons, thereby leading to further electron removal from the target by autoionization.

In summary, we have measured the fragmentation branching ratios and the KER distributions that result from collisions between CO and slow C^{6+} or Ar^{11+} ions and compared

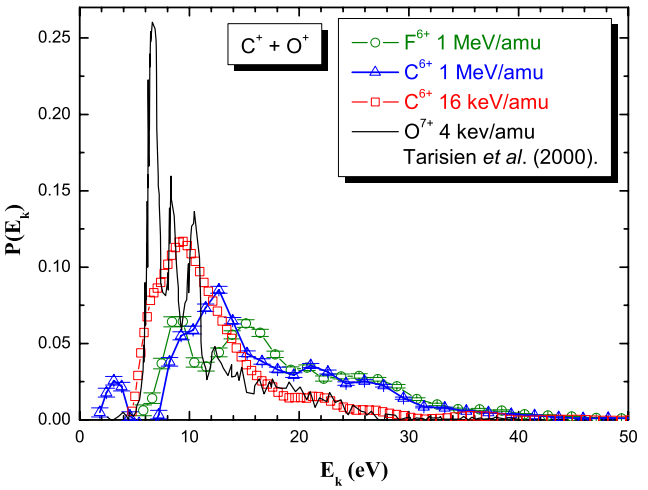

FIG. 3. (Color online) $C^+ + O^+$ KER distributions resulting from collisions with a range of projectile $\frac{q}{v}$. The high velocity results, in which electrons are removed by ionization, are from Ref. [19], while the O^{7+} results are from Tarisien *et al.* [27].

the results to those obtained with faster projectiles. Fragmentation branching ratios are fairly constant for all these soft collisions, namely electron capture by slow HCI and ionization by fast HCI, over a wide range of projectile charges and velocities. This was attributed to the multielectron nature of the target. In contrast, the KER distributions vary considerably and therefore can give insight into the excited electronic states of the intermediate molecular ion. Both the experimental results and our EOBM calculations suggest that multiple-electron capture results in the population of projectile states that rapidly autoionize.

This work was supported by Research Corporation and by the Chemical Sciences, Geosciences and Biosciences Division, Office of Basic Energy Sciences, Office of Science, U.S. Department of Energy.

[1] R. J. Mawhorter *et al.*, Phys. Rev. A **75**, 032704 (2007).
[2] R. F. Elsner *et al.*, J. Geophys. Res. **110**, A01207 (2005).
[3] V. Kharchenko *et al.*, Geophys. Res. Lett. **33**(11), L11105 (2006).
[4] J. B. Greenwood, I. D. Williams, S. J. Smith, and A. Chutjian, Phys. Rev. A **63**, 062707 (2001).
[5] T. E. Cravens, Science **296**, 1042 (2002).
[6] V. A. Krasnopolsky, J. B. Greenwood, and P. C. Stancil, Space Sci. Rev. **113**, 271 (2004).
[7] C. M. Lisse *et al.*, Astrophys. J. **635**, 1329 (2005).
[8] B. J. Wargelin and J. J. Drake, Astrophys. J. **578**, 503 (2002).
[9] A. Dalgarno and S. Lepp, in *Atomic, Molecular, and Optical Physics Handbook*, edited by G. F. W. Drake (AIP Press, Woodbury, New York, 1996).
[10] P. D. Feldman and W. H. Brune, Astrophys. J. **209**, L45 (1976).
[11] P. Eberhardt *et al.*, Astron. Astrophys. **187**, 484 (1987).
[12] D. M. Hunten *et al.*, in *Saturn*, edited by F. Vilas, C. R. Chapman, and M. S. Matthews (University of Arizona Presss, Tucson, 1988).
[13] V. A. Krasnopolsky, B. R. Sandel, F. Herbert, and R. J. Vervack, J. Geophys. Res. **98**, 3065 (1993).
[14] A. O. Nier, Int. J. Mass Spectrom. Ion Phys. **66**, 55 (1985).
[15] *Electron-Impact Ionization*, edited by T. D. Märk and G. H. Dunn (Springer, New York, 1985).
[16] P. Beiersdorfer, M. Bitter, M. Marion, and R. E. Olson, Phys. Rev. A **72**, 032725 (2005).
[17] I. Ben-Itzhak, S. G. Ginther, and K. D. Carnes, Phys. Rev. A **47**, 2827 (1993).
[18] I. Ben-Itzhak, S. G. Ginther, V. Krishnamurthi, and K. D. Carnes, Phys. Rev. A **51**, 391 (1995).
[19] V. Krishnamurthi, I. Ben-Itzhak, and K. D. Carnes, J. Phys. B **29**, 287 (1996).
[20] E. Wells *et al.*, Phys. Rev. A **72**, 022726 (2005).
[21] H. O. Folkerts *et al.*, J. Phys. B **30**, 5833 (1997).
[22] G. Sampoll *et al.*, Phys. Rev. A **45**, 2903 (1992); K. Wohrer *et al.*, *ibid.* **46**, 3929 (1992).
[23] J. Vancura and V. O. Kostroun, Phys. Rev. A **49**, 321 (1994).
[24] R. L. Watson, G. Sampoll, V. Horvat, and O. Heber, Phys. Rev. A **53**, 1187 (1996).
[25] H. O. Folkerts, R. Hoekstra, and R. Morgenstern, Phys. Rev. Lett. **77**, 3339 (1996).
[26] H. O. Folkerts *et al.*, J. Phys. B **30**, 5849 (1997).
[27] M. Tarisien *et al.*, J. Phys. B **33**, L11 (2000); L. Adoui *et al.*, Phys. Scr., T **T62**, 89 (2001).
[28] J. Rajput and C. P. Safvan, Phys. Rev. A **75**, 062709 (2007).
[29] N. A. Schwadron and T. E. Cravens, Astrophys. J. **544**, 558 (2000).
[30] H. A. Bethe and R. Jackiw, *Intermediate Quantum Mechanics*, 3rd ed. (Benjamin/Cummings, Menlo Park, CA, 1986), Chap. 19.
[31] I. Ali *et al.*, Phys. Rev. A **64**, 022712 (2001).
[32] P. Sobocinski *et al.*, J. Phys. B **35**, 1353 (2002), and references therein.
[33] F. Frémont *et al.*, Int. J. Mol. Sci. **3**, 115 (2002).
[34] I. Ben-Itzhak, S. G. Ginther, and K. D. Carnes, Nucl. Instrum. Methods Phys. Res. B **66**, 401 (1992).
[35] E. Wells *et al.*, Nucl. Instrum. Methods Phys. Res. B **241**, 101 (2005).
[36] M. P. Stöckli *et al.*, Rev. Sci. Instrum. **67**, 1162 (1996).
[37] W. C. Wiley and I. H. McLaren, Rev. Sci. Instrum. **26**, 1150 (1955).
[38] A. Remscheid *et al.*, J. Phys. B **29**, 515 (1996).
[39] See EPAPS Document No.E-PLRAAN-77-093806 for data on the KER distributions of the various fragmentation channels. The EPAPS material contains relative cross section data similar to that shown in Table I for $v=0.39$ a.u. $Ar^{11+}+CO$ and $v=9.85$ a.u. $Ar^{14+}+CO$ collisions. In addition, it contains kinetic energy release distributions $[P(E_k)$ plots] for all statistically significant dissociation channels of CO after collisions with the C^{6+} at $v=0.8$ a.u. and Ar^{11+}at $v=0.39$ a.u. projectiles. For more information on EPAPS, see http://www.aip.org/pubservs/epaps.html.
[40] A. Niehaus, J. Phys. B **19**, 2925 (1986).